Decentralized frequency-voltage control and stability enhancement of standalone wind turbine-load-battery

Reza Hemmati [1], Neda Azizi [1], Miadreza Shafie-khah [2], João P. S. Catalão [2,3,4,*]

[1] Department of Electrical Engineering, Kermanshah University of Technology, Kermanshah, Iran

[2] C-MAST, University of Beira Interior, 6201-001 Covilhã, Portugal

[3] INESC TEC and Faculty of Engineering of the University of Porto, 4200-465 Porto, Portugal

[4] INESC-ID, Instituto Superior Técnico, University of Lisbon, 1049-001 Lisbon, Portugal

* Corresponding author at Faculty of Engineering of the University of Porto, R. Dr. Roberto Frias, Porto, Portugal.

E-mail address: catalao@ubi.pt (J.P.S. Catalão).

Abstract

This paper simulates an islanding network including wind turbine, battery energy storage systems (BESS), and load. The purpose is to control voltage and frequency of the load following wind speed variations by proper control of BESS. A decentralized control scheme including two control loops is designed on BESS. One control loop is implemented for voltage regulation and the other loop is designed for frequency control. Both loops are equipped with PI (Proportional–Integral) type controllers as internal controllers. Furthermore, both loops are equipped with supplementary stabilizers as external controllers. The internal controllers regulate frequency and voltage and the external stabilizers enhance stability. This paper optimally tunes all the parameters of internal controllers and external stabilizers at the same time. The problem for tuning a large number of the design variables is mathematically expressed as a mixed integer nonlinear optimization programming and solved by modified-adaptive PSO technique. The proposed methodology is simulated on a typical standalone network including wind turbine, BESS, and load. The accurate model of BESS and wind turbine is incorporated to cope with real conditions. Moreover, in order to demonstrate the real-world results, non-linear time domain simulations are carried out in MATLAB software. The results verify that the proposed control scheme can efficiently utilize BESS to control voltage, regulate frequency, and damp out oscillations under wind and load variations.

Keywords:

Battery Storage System; Decentralized Frequency-Voltage Control; Induction Generator; Standalone Wind Turbine.

Nomenclature

Parameters and symbols	
A	Turbine swept area (m2)
c_p	Performance coefficient of the turbine
c_{p_pu}	Performance coefficient in pu of the maximum value of c_p
F	Frequency (Hz)
k_p	Power gain for c_{p_pu}=1 pu and v_{wind_pu}=1 pu, k_p is less than or equal to 1
P_m	Mechanical output power of the turbine (W)
P_{m_pu}	Power in pu of nominal power for particular values of ρ and A
Tm	turbine torque output
V	Voltage (pu)
V_{wind}	Wind speed (m/s)
V_{wind_pu}	Wind speed in pu of the base wind speed
ρ	Air density (kg/m^3)
β	Blade pitch angle (deg)
λ	Tip speed ratio of the rotor blade tip speed to wind speed

1. Introduction

In the recent years, wind energy has shown rapid growth as a clean and inexhaustible energy source at all around the world [1]. Over year 2015, 63.5 GW new wind power generation has been added to the power grid worldwide, increasing the cumulative wind energy power to 432.9 GW. It is anticipated that by 2030, the total cumulative wind power installed worldwide reaches 1430-1933 GW [2]. However, as the penetration levels increases, it is of considerable concern that fluctuating output power of wind farms will affect the operation of the interconnected grids especially weak power systems [3, 4]. Such cases may require some measures to smooth the output fluctuations to have a reliable power system [5, 6]. Wind energy has many benefits, but

high penetration of wind power can introduce technical challenges about grid interconnection, power quality, reliability, protection, generation dispatch, and control [7-9].

The voltage and frequency regulations are the main problems regarding control of wind turbines [10]. In wind generating system, the input mechanical power to the wind turbine changes together with wind speed variations. As a result, the electrical power produced by wind generating system comprises voltage-frequency fluctuations [11]. Such generating system cannot be connected to the electrical grid, because of its frequency-voltage fluctuations [12]. It cannot moreover supply the standalone loads, because the voltage and frequency of the load would change together with variations of load demand [12]. For instance, without proper control on voltage and frequency in the standalone mode, the voltage and frequency will decrease together with increment of load demand and they will raise accompanied by reduction of load demand [12]. As a result, a proper control is required to make the wind generating system practical in both connected to the grid [13] or standalone operation [14]. In other words, the output voltage produced by wind generators must be regulated in terms of magnitude and frequency [12].

In the standalone operation, it is necessary to present proper control strategy for wind generators to control power, voltage, and frequency [15]. The control strategy makes significant impacts on the performance of generator and interfacing converter [15, 16]. Different types of generators such as induction generator and permanent magnet synchronous generator (PMSG) can be installed to the wind turbines [17, 18]. In the standalone variable-speed wind turbine installed with PMSG, load-side converter regulates the magnitude and frequency of AC voltage and the DC voltage. On the other hand, the generator-side inverter is controlled to extract the optimal energy of wind [17, 18]. Different control methods have already been applied to improve the performance of variable-speed wind turbine on the standalone operation [19].

In the above-mentioned references, various control strategies are presented to regulate both the frequency and voltage. Where, the control loops are implemented by internal controllers (such as PI type controllers) to regulate the frequency and voltage. However, these studies do not provide a separate controller (or stabilizers) to damp out the oscillations and stability improvement. In other words, they have only designed the internal controllers to regulate the frequency and voltage. Although some works have enhanced the stability of the network, this stability enhancement has not been addressed by a separate stabilizer on the control loops. As a result, current paper aims at designing separate controllers (i.e., stabilizers) in addition to the internal controllers for frequency and voltage regulation as well as stability enhancement.

One of the proper methods to cope with wind fluctuations is to utilized energy storage systems (ESS) (especially battery energy storage systems (BESS)) together with stand-alone wind units [20, 21]. Similar to the renewable energy, energy storage systems (ESSs) [22] are one of the most suitable technologies in electric power systems that provide technical and economic advantages. There are several methods for storing energy such as mechanical, electro-chemical, electrical, thermal, and chemical approaches. Battery storage systems are also one of the most relevant technologies of energy storage systems that have attracted much attention in the recent years. BESS store electrical energy in the form of electrochemical process, and then the stored energy can be restored and sent back to the network. Some of the BESS applications for wind farms involve a simple scheme to charge and discharge the BESS, such as storing excess power, if the wind power output exceeds a threshold [23].

The BESS can successfully control both active and reactive powers independent of each other. In such decoupled P-Q control system, both active and reactive powers can be controlled in both directions as well as independent of each other. The decoupled P-Q control on BESS can also be

supported by supplementary stabilizers to enhance network stability. The active and reactive powers have direct correlation with frequency and voltage, receptively. As a result, the P-Q control can also be implemented as decentralized frequency-voltage control system [24]. In [24], the acceptable ranges of frequency and voltage are considered as the constraints of optimization problem and the network stability is improved by such modelling.

With respect to the above conducted literature review, this paper presents a new control strategy on standalone battery-wind-load system in order to frequency-voltage control and stability enhancement at the same time. In the proposed structure, the frequency and voltage of the load are regulated by decoupled F-V control on BESS. The control loops of BESS are also equipped with supplementary stabilizers to damp out the oscillations and stability enhancement.

Although decoupled P-Q control and frequency-voltage control [24] have already been investigated by the researchers, this paper is different from the above references. In [25], the decoupled P-Q control is presented on BESS in order to regulate P (active power) and Q (reactive power) between BESS and network. But this paper presents a decupled frequency-voltage control on BESS in order to control a wind turbine. In [25], the network is not integrated with wind turbine and they do not discuss modelling and control of wind turbines. Whereas, the current paper models and discusses the wind turbine, and utilizes BESS to support the wind turbine in the standalone mode. On the other hand, the frequency-voltage control is addressed by [24] and this work also enhances the stability of the network. But reference [24] does not design a separate controller for stability enhancement and it presents an intelligent methodology to tune the internal controllers of BESS for stability improvement. However in the current paper, separate controllers (i.e., supplementary stabilizers) are designed in addition to the internal

controllers. The proposed supplementary stabilizers are mounted on the internal control loops and they enhance the network stability.

In summary, the main contributions of the current work can be highlighted as follows;

- ✓ A decoupled frequency-voltage control on BESS is presented in order to control wind turbines. The decoupled frequency-voltage control on BESS has already been studied. But, this paper installs supplementary stabilizers on the decoupled frequency-voltage loops to enhance network stability. This is one of the main contributions of the paper. It is worth mentioning that some papers have already addressed the decoupled frequency-voltage control and stability enhancement by BESS at the same time. But they do not utilize the supplementary stabilizers on BESS. As a result, the current paper addresses a novel structure for decoupled frequency-voltage control and stability enhancement by BESS.
- ✓ The proposed decoupled frequency-voltage control and supplementary stabilizers are modelled and simulated to control wind turbines. Such structure has not been addressed on wind turbines. The decoupled frequency-voltage control has already been simulated on wind turbines. But the proposed structure including supplementary stabilizers has not been studied.
- ✓ The proposed structure regulates voltage, controls frequency, and enhances stability at the same time in the standalone wind-BESS-load system.
- ✓ All the internal controllers (voltage and frequency controllers) and supplementary stabilizers are tuned at the same time by PSO algorithm. This is also one of the main contributions of the paper. Because all the internal controllers and stabilizer are simultaneously tuned to find the most optimal operating condition of the network. The

proposed methodology results in the best operation for the whole system including BESS, wind turbine, and load.

- ✓ In order to cope with real conditions, the real models of wind turbine and converter are derived and simulated. The real world modelling and nonlinear time-domain simulations are carried out in MATLAB software.

2. Network under study as test case

2.1. Network structure

Single-line diagram of the network under study is depicted in Figure 1. The initial network is given from MATLAB Simulink software [26], but it has been modified in this paper. As it is seen, the battery energy storage system is connected to the network through a three-phase inverter. The standalone network consists of asynchronous generator, load, and wind turbine.

In this paper, all simulations are carried out in MATLAB software. The model of components such as wind turbine, generator, and battery are taken from MATLAB library. The Nickel-Cadmium battery is chosen from MATLAB library and its accurate model can be found in MATLAB software manual.

It is worth mentioning that the test network shown in Figure 1 is only opted as an illustrative test case and the proposed strategy (decentralized V-F control or P-Q control) can also be simulated on the other test networks as shown in [28-30]. In the current paper, the purpose is to control the voltage and frequency of wind turbine in standalone operation and the network shown in Figure 1 is proper for such purpose. However, the proposed control strategy can also be simulated on the other networks with different structures and including or excluding wind turbines.

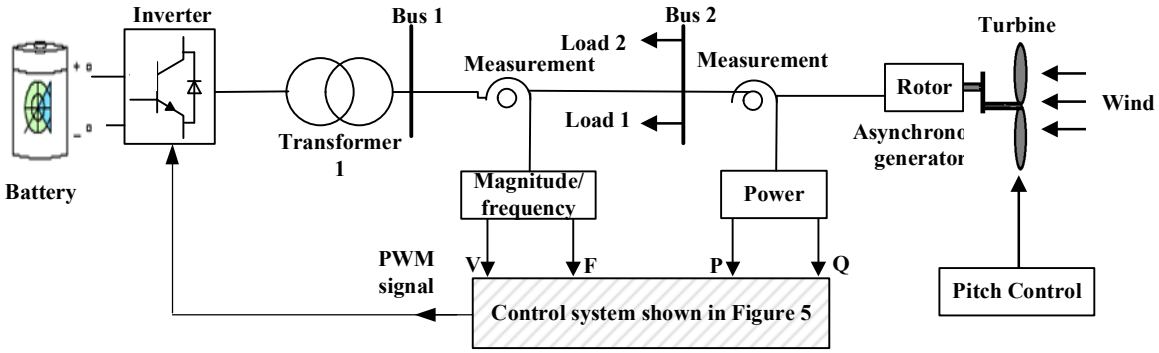

Figure 1: Schematic of the test system

2.2. Wind turbine and asynchronous generator

The model of wind turbine and generator is based on the steady-state power characteristics of the turbine. The output power of the turbine is given by (1) [26], and it can also be normalized in the per-unit as (2).

$$p_m = c_p(\lambda,\beta)\frac{\rho A}{2}V_{wind'}^3 \tag{1}$$

$$P_{m\_pu} = k_p c_{p\_pu} V_{wind\_pu'}^3 \tag{2}$$

A generic equation is used to model $c_p(\lambda,\beta)$ as (3) [13].

$$c_p(\lambda,\beta) = c_1(c_2/\lambda_i - c_3\beta - c_4)e^{-c_5/\lambda_i} + c_6\lambda \tag{3}$$

where,

$$\frac{1}{\lambda_i} = \frac{1}{\lambda + 0.08\beta} - \frac{0.035}{\beta^3 + 1} \tag{4}$$

The model of such wind turbine is shown in Figure 2 [26].

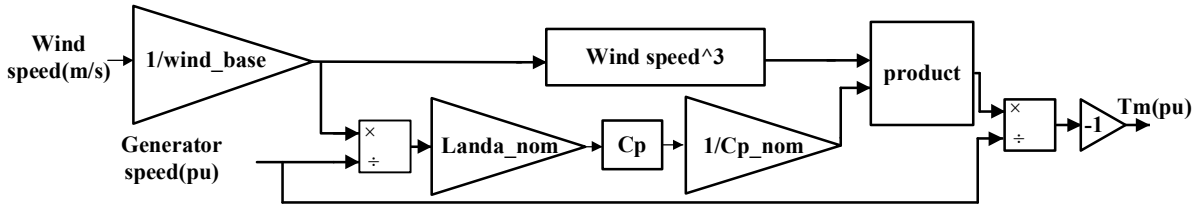

Figure 2: Wind turbine model

Figure 3 shows the wind turbine and the induction generator (WTIG). The stator winding is connected to the local load, and the rotor is driven by the wind turbine. The induction generator converts the power got by wind turbine into electrical energy and sends it to the load through the stator winding. In order to limit the generator output power on the nominal value under high wind speeds, the pitch angle is controlled. The induction machine needs to operate slightly above the synchronous speed to work on the generation mode. The speed variation is typically so small, and WTIG is considered a fixed-speed wind generator. The reactive power absorbed by the induction generator can be provided by reactive sources such as capacitor banks.

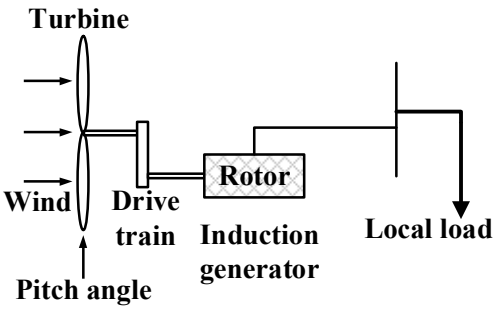

Figure 3: Wind turbine and the induction generator

The electrical output power produced by wind unit is limited to the nominal power by blade pitch angle control as depicted in Figure 4. It is clear that a proportional-Integral (PI) controller is utilized to control the blade pitch angle. While the electric output power of wind turbine is below the rated power, the pitch angle is fixed to zero degree. When the output power produced by the wind turbine increases more than the rated power, the controller increases the pitch angle until reduction of power below the rated level [27].

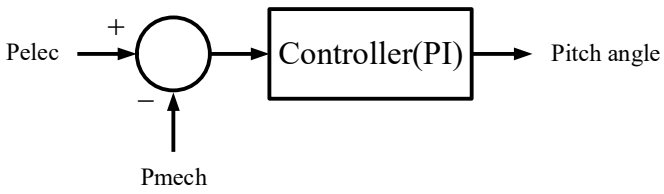

Figure 4: Mechanical controller of wind turbine for blade pitch angle control

2.3. Controllers and stabilizers

Figure 1 shows a block as control system. The structure of this control system is depicted in Figure 5. The proposed structure comprises two control loops. One control loop is designed for frequency regulation. In this loop, the network frequency is compared against set-point value of frequency and the error is fed into internal PI controller. The other loop regulates the voltage and it compares the network voltage against set-point value of voltage and the error is fed into an internal PI controller. At the output of internal PI controllers, the dqo components are transferred to abc frame in order to make PWM signal for BESS operation. Eventually, the generated PWM signal is sent to the converter between battery and network as shown in Figure 1.

In Figure 5, the internal PI controllers (i.e., tracking controllers) are applied to follow the reference values (i.e., set point) of the control loops, and the supplementary stabilizers (i.e., damping or regulatory controllers) are utilized to damp out the oscillations and to improve network stability. Each stabilizer includes gain, washout filter, and lead-lag compensators. The washout filter is applied to filter the steady-state offset in the output, and T_w indicates its time constant. The gain and lead-lag blocks make a dynamic compensator including four time constants (i.e., T_1–T_4), and an additional gain (i.e., K_{DC}). The stabilizer on the active power loop (i.e., frequency control loop) produces an electrical torque in phase with the rotor speed deviations and damps out the active power oscillations (i.e., frequency oscillations). Similarly, the output of the stabilizer on the reactive power control loop (i.e., voltage control loop) is proportional to the voltage deviations and damps out the reactive power oscillations (i.e., voltage oscillations).

The main contribution of this paper is to add two supplementary stabilizers to internal control loops as shown in Figure 5. Where, one supplementary stabilizer is integrated into frequency control loop and the other supplementary stabilizer is integrated into voltage control loop. In the proposed structure, the internal PI controllers regulate the frequency and voltage and the supplementary stabilizers enhance network stability. All the controllers and stabilizers are tuned and designed at the same time by PSO algorithm.

The proposed control structure is called a decentralized voltage-frequency control, because the control loops of voltage and frequency are separated from each other. In other words, the control loops operate independent of each other and they do not make impact on each other. As a result, it is possible to control the frequency subject to constant voltage and vice versa. The decentralized control is also known as decoupled control and it is commonly used in the robust control techniques.

This paper only models and analyses the transient and dynamic operation of BESS, and it does not discuss the steady-state operation. The charging and discharging states often take several hours to be completed. For instance, a battery with 100 kWh capacity and 10 kW rating power takes more than 10 hours to be completely charged, and it also takes several hours for fully discharging. In this paper, such long-term simulations are not discussed, and the purpose is to study the transient operation of BESS under disturbances. The ability of BESS in controlling voltage and frequency is simulated. When the BESS gets the charging command, it starts charging energy. After a fully charged, the charging power drives towards zero and the charging state is finished. The command for charging can be from state of charge (SOC) controllers or from the operator (manual operation). This paper does not deal with this issue and does not model and discuss SOC controllers. In other words, it is assumed that there is a command to

charge, now the purpose is to design a proper control structure to cope with such command signal and utilize the BESS according to the command with the best possible transient operation. For instance, when BESS is aimed to control the frequency, the set point of the control loop on the BESS is tuned on the desired level, and the BESS changes its active power to control the frequency according to the set point signal. It is assumed that the set point signal of the control loop is available. The purposes are (i) improve transient operation of BESS, (ii) track the set point signal and fix the frequency and voltage on the desired levels. As a result, this paper does not design a separate controller for SOC. In order to design a proper controller for SOC, an extra control structure can be added to the proposed control strategy for SOC control. The SOC control can regulate the charged and discharged power subject to capacity of the battery (kWh) and rated power of inverter (kW).

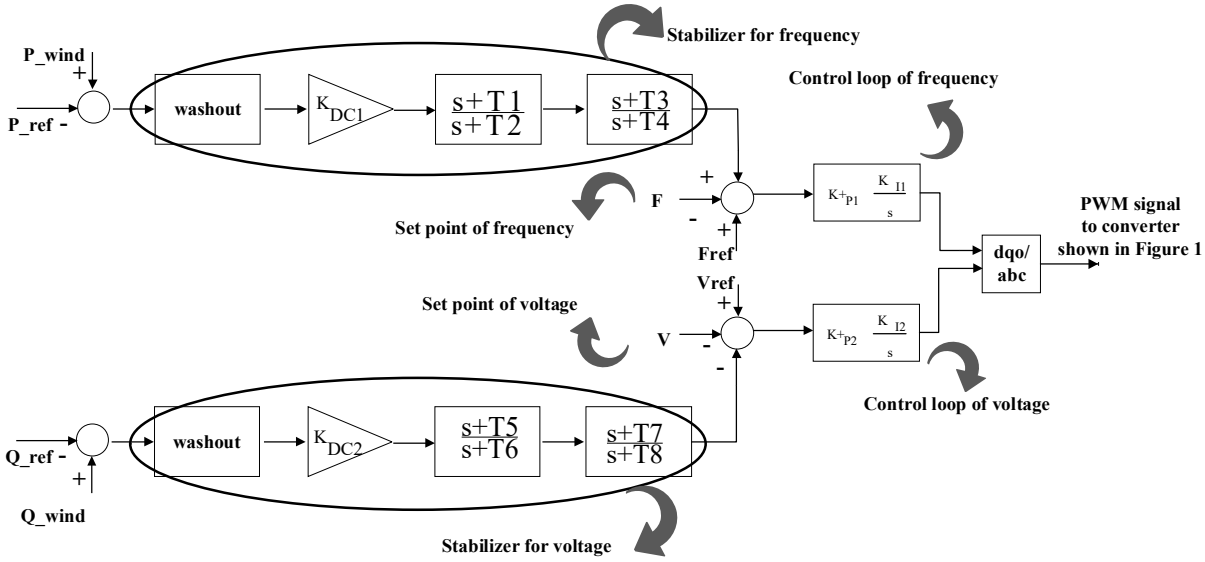

Figure 5: Structure of the proposed control strategy

3. Mathematical formulation

The objective function of the proposed problem is introduced as (5) that is Integral of the Time multiplied Absolute Error (ITAE), and it calculates the area under the curve following oscillations. As a result, the problem for tuning controllers is expressed through (6) to (14) which is a constrained nonlinear optimization programming. In this problem, the objective function (6) reveals oscillations of frequency and voltage which should be minimized. Constraints (7) to (10) indicate the boundaries on the proportional and integral gains of PI controllers. Constraints (11) to (14) indicate the boundaries on the stabilizers. This problem is solved by PSO algorithm, and its detail can be found in [25] and the solution methodology is discussed in the next subsection.

$$\mathrm{ITAE} = \int_0^t t|\Delta f|dt + \int_0^t t|\Delta V|dt \tag{5}$$

Min (ITAE) (6)

Subject To:

$K_{P1}^{min} < K_{P1} < K_{P1}^{max}$ (7)

$K_{P2}^{min} < K_{P2} < K_{P2}^{max}$ (8)

$K_{I1}^{min} < K_{I1} < K_{I1}^{max}$ (9)

$K_{I2}^{min} < K_{I2} < K_{I2}^{max}$ (10)

$K_{DC1}^{min} < K_{DC1} < K_{DC1}^{max}$ (11)

$K_{DC2}^{min} < K_{DC2} < K_{DC2}^{max}$ (12)

$T_i^{Min} < T_i < T_i^{Max}, i \in [1,4]$ (13)

$T_j^{Min} < T_j < T_j^{Max}, j \in [5,8]$ (14)

3.1. Solution algorithm

This paper finds optimal values of PI controllers (i.e., K_{P1}, K_{P2}, K_{I1}, K_{I2}) and stabilizers (K_{DC1}, K_{DC2}, T_1 to T_8) by modified PSO technique. PSO algorithm is a well-known optimization problem which has been widely applied to solve different continuous, discrete, mixed integer,

integer, liner, and nonlinear optimization problems [28, 29]. It can also be used to solve the constrained optimization problems [30]. The details of this algorithm are given in [31].

In this paper, the conventional PSO algorithm has been modified and improved and modified-adaptive PSO is presented. In the proposed modified-adaptive PSO technique, weighing factor is linearly decreased from one towards zero resulting in adaptive performance for the algorithm. As well, the specifications of genetic algorithm such as crossover and mutation are included in PSO technique to modify its search. As a result, this algorithm is an advanced version of conventional PSO algorithm.

Figure 6 shows the flowchart for solution of the proposed problem by modified adaptive PSO. First, input data of the problem are fed into the algorithm and the initial population is randomly generated. Then, one particle in the population is selected for evaluation. Each particle comprises one possible solution of the problem. In other words, each particle includes 14 design variables related to the optimal values of PI controllers (four parameters: K_{P1}, K_{P2}, K_{I1}, K_{I2}) and stabilizers (ten parameters: K_{DC1}, K_{DC2}, T_1 to T_8). At next step, the contents of the selected particle are set on the PI controllers and stabilizers and constraints (7) to (14) are checked. If the constraints are violated, the selected particle is removed and next particle in the population is selected for evaluation. Afterward, objective function (6) is calculated for the qualified particles and the particle with minimum objective function is determined as the best particle of current iteration. After each iteration, the convergence of PSO algorithm is checked. If the convergence criterion is not met, the next iteration is started until convergence of algorithm. At each iteration, the best particle is determined as the local optimal and the best particle related to all iterations (the best particle among all locals optimal) is selected as global optimal. These local optimal and global optimal particles are used to update the population at each iteration. Eventually after

convergence of algorithm, the best particle under all iterations is achieved. The contents of this particle are the optimal values of PI controllers (i.e., K_{P1}, K_{P2}, K_{I1}, K_{I2}) and stabilizers (K_{DC1}, K_{DC2}, T_1 to T_8). The details about updating the population, convergence criterion, structure of population and their formulation can be found in [32].

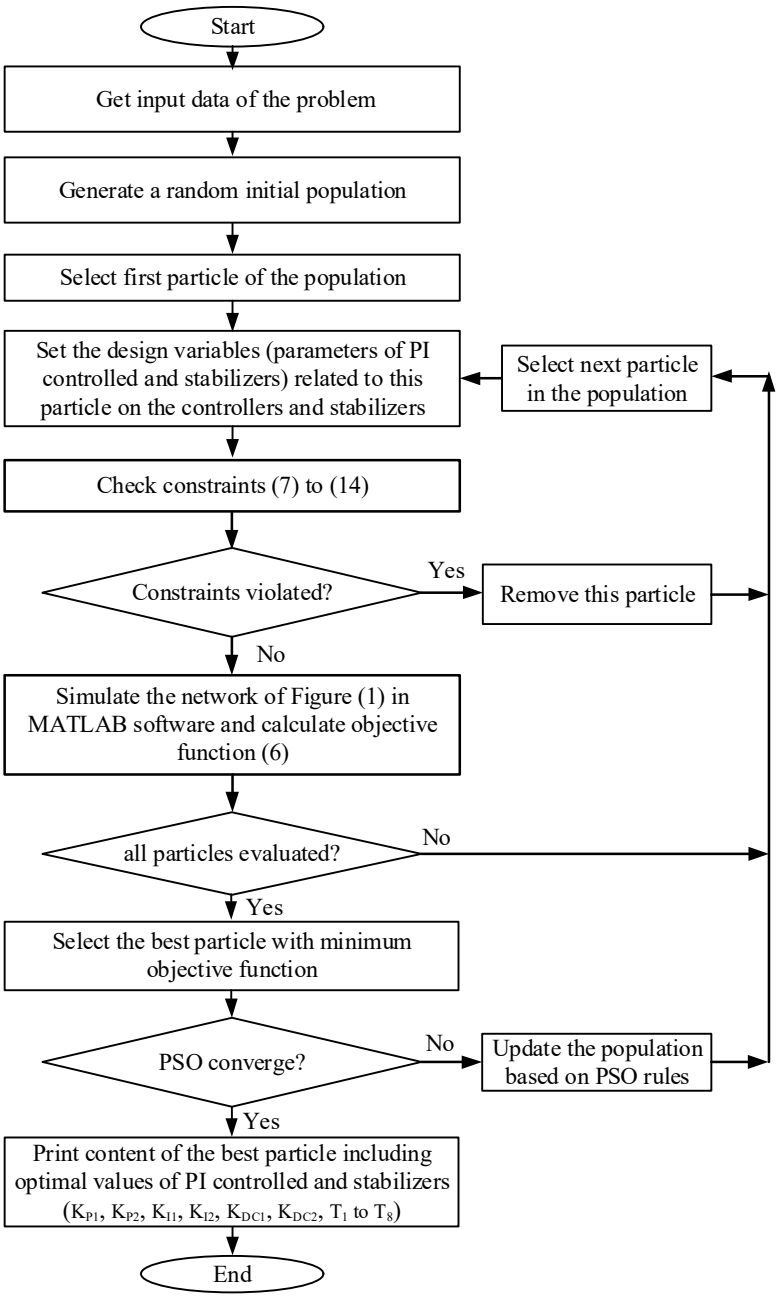

Figure 6: Flowchart showing solution of the proposed problem by PSO technique

4. Data of the problem

Test system parameters are listed in Table 1 including parameters of the asynchronous generator, wind turbine, transformer, and load. The limitations on the parameters of the controllers and stabilizers are also listed in Tables 2 and 3. DC voltage of the battery is 500 (V), and wind speed is 10m/s. The acceptable range of voltage is between 0.9 p.u. and 1.1 p.u. (±10% variations is allowed). The acceptable range of frequency is between 59.5 Hz and 60.5 Hz under islanding operation. Under transient and contingency condition, the frequency is allowed to range between 47 and 55 Hz.

Table 1: Parameters of test system

Generator 1	Transformer 1	Load 1	Load 2
P_n=275VA v_n=480V f_n=60Hz	ΔY-g, V1 ph-ph (Vrms)=208v R1(p.u.)=0.002 X1(p.u.)=0.04 V2 ph-ph (Vrms)=480v R2(p.u.)=0.002 X2(p.u.)=0.04	Pload=0kW Qc=22kvar	Pload=50k Q=0 kvar

Table 2: Parameters of controllers

controller for frequency control		controller for voltage control	
Minimum	Maximum	Minimum	Maximum
K_{P1}=0.00001	K_{P1}=0.0005	K_{P2}=0.00001	K_{P2}=0.0005
K_{I1}=0.1	K_{I1}=5	K_{I2}=10	K_{I2}=30

Table 3: Parameters of stabilizers

stabilizer for frequency control		stabilizer for voltage control	
Minimum	Maximum	Minimum	Maximum
T_1=0.15	T_1=0.25	T_5=0.3	T_5=0.5
T_2=0.001	T_2=0.02	T_6=0.001	T_6=0.02
T_3=0.001	T_3=0.005	T_7=0.001	T_7=0.005
T_4=0.001	T_4=0.02	T_8=0.001	T_8=0.02

5. Results and discussions

5.1. Tuning of the parameters

The parameters of the controllers and stabilizers are tuned by PSO algorithm, and the results are listed in Table 4. It is clear that 14 parameters are optimally tuned. It is worth mentioning that the current problem is solved by various optimization techniques and they are compared to each other. Eventually, modified adaptive PSO finds the solution sooner than the other techniques and it is selected to solve the problem. After solving the problem by several optimization algorithms and taking one similar response, it is confirmed that the achieved solution is the global optimal solution. Meanwhile, each algorithm is performed several times to guarantee its output. The setting of the algorithm is also changed and the problem is solved under various setting to prevent falling into local optimums.

Table 4: Parameters of PI controllers and stabilizers

	Parameter	Optimal value
Proportional gains	K_{P1}	0.0002
	K_{P2}	0.0002
Integral gains	K_{I1}	1.98
	K_{I2}	19.8
Auxiliary gains of the stabilizers	K_{DC1}	0.0020
	K_{DC2}	0.0079
Time constants of the stabilizers	T1	0.190
	T2	0.010
	T3	0.001
	T4	0.010
	T5	0.410
	T6	0.010
	T7	0.001
	T8	0.010

5.2. Decoupled frequency and voltage regulation

The main purpose of the proposed control structure is to control both frequency and voltage independent of each other. In this regard, two different simulations are carried out to demonstrate

the capability of the introduced method for frequency control subject to constant voltage and voltage regulation subject to fixed frequency.

The first purpose is to investigate capability of the control structure to change frequency while it maintains the voltage on the reference level. In this regard, set point of frequency control loop is altered from 60 to 60.1 at second 1.5. The results following such disturbance as depicted in Figure 7. In this figure, the set points of the control loops are depicted by dashed lines. It is clear that the frequency increases from 60 to 60.1 while the voltage is kept on the reference level following disturbance. The results demonstrate that the frequency control loop can successfully track its set point value while it does not make on the voltage control loop. The voltage control loop shows oscillations following disturbance and it drives back to the nominal value following alterations.

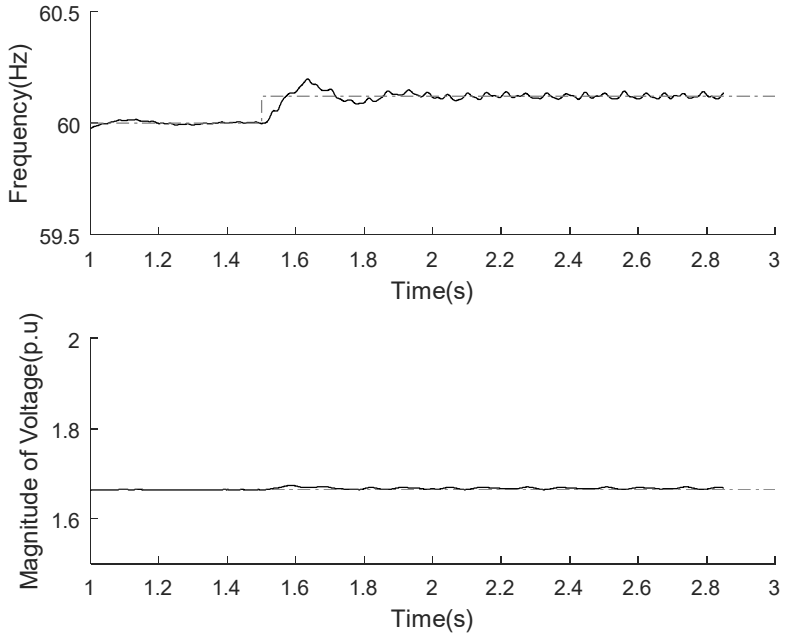

Figure 7: Frequency and voltage of load after changing set point of frequency (the set points of the control loops are depicted by dashed lines)

The next simulation is carried out to demonstrate capability of the control strategy to change voltage and maintaining frequency on the set point level. In this regard, set point of voltage control loop is changed from 1.68 to 1.95 at second 1.5. Figure 8 depicts the results following this disturbance and the set points of the control loops are depicted by dashed lines. It is demonstrated that the proposed control structure can efficiently change the voltage magnitude while it maintains the frequency on the set point level. After disturbance at second 1.5, the voltage tracks the set point level and increases from 1.68 to 1.95. On the other hand, the frequency goes back to set point level following alterations.

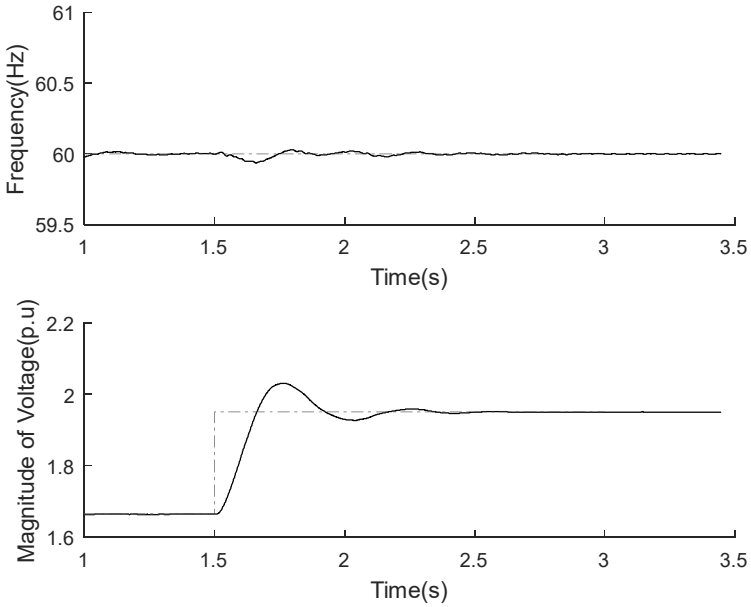

Figure 8: Frequency and voltage of load after changing set point of voltage (the set points of the control loops are depicted by dashed lines)

5.3. Operation under variable wind speed and variable load

The proposed control strategy is able to control both the frequency and voltage of the load under variable wind speed and variable load demand. In order to demonstrate this capability, wind speed is changed from 10 m/s to 15 m/s at second 2 and Figure 9 shows the results following

wind speed variations. It is clear that both the frequency and voltage of the load are kept on the set point levels (nominal levels) following disturbance and they drive back to the nominal values after oscillations. As a result, the proposed control strategy on BESS can successfully regulate both the frequency and voltage of the load by proper utilization of the BESS. Figure 10 also shows the frequency and voltage of load following successive wind speed alteration at seconds 2 and 4. It is clear that the frequency and voltage are efficiently controller under such situation.

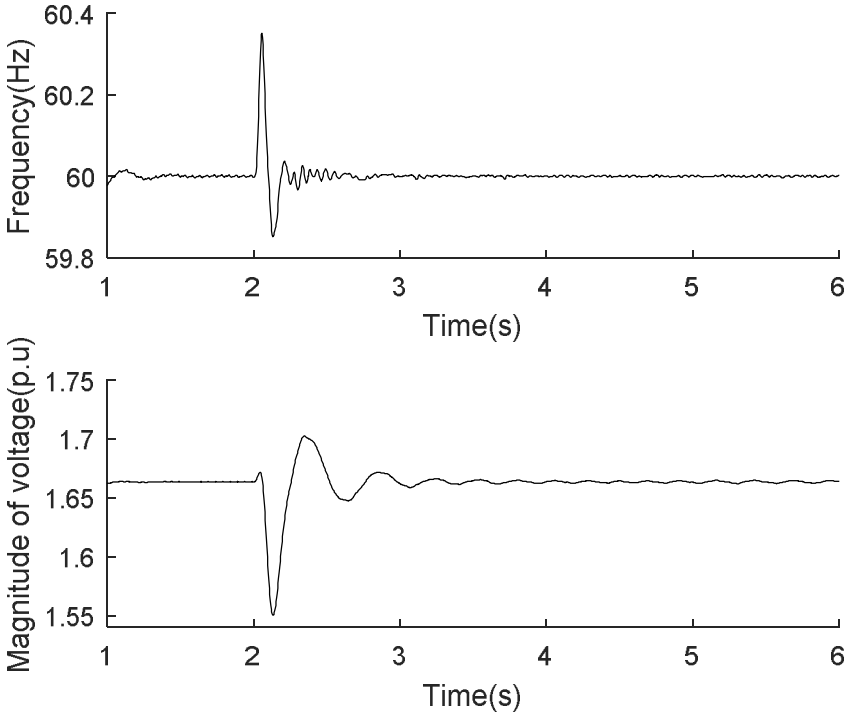

Figure 9: Frequency and voltage of load following wind speed alteration at second 2

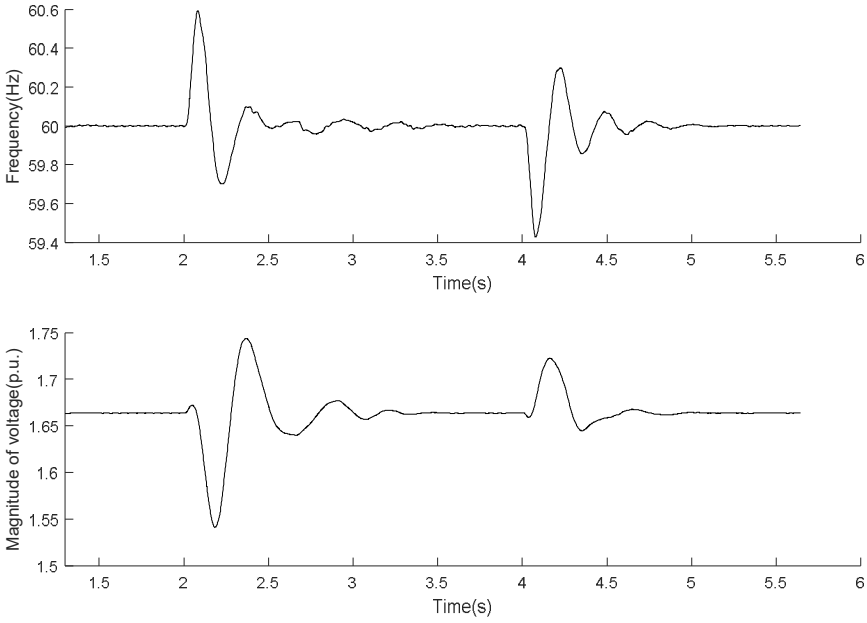

Figure 10: Frequency and voltage of load following successive wind speed alteration

The other capability of the proposed methodology is kept both the frequency and voltage of the load under variable load demand. In this regard, load of the network is increased by 20% at second 3 and results are presented in Figure 11. The results verify that the proposed controller strategy on BESS can efficiently utilize BESS to keep the frequency and voltage of the load on the nominal levels following variable load demand.

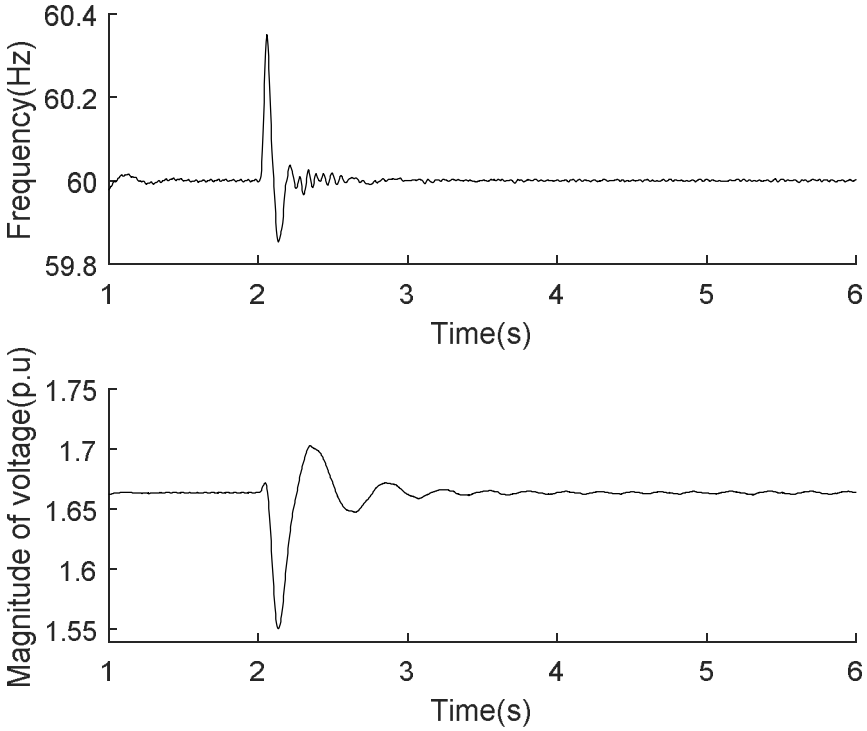

Figure 11: Frequency and voltage of load following load increment by 20% at second 3

5.4. Operation with and without BESS

In the previous sections, proper control on BESS successfully utilized BESS to control both the frequency and voltage under wind and load variations. In order to demonstrate the impacts of BESS on the operation of network, two cases are simulated and compared including the network with BESS (i.e., BESS-wind turbine-load) and the network without BESS (i.e., wind turbine - load).

Figure 12 shows the frequency of the load with and without BESS following changing load at second 2. In the network without BESS, the frequency cannot drive back to the reference level and there is a steady-state error in the network frequency. On the other hand in the network with BESS, the frequency is kept constant on the reference level following disturbance. The network with BESS not only can keep the reference on the reference level, but also it shows less

oscillations in the frequency following disturbance. As per Figure 12, the oscillations of frequency in the network with BESS are significantly less than the network without BESS.

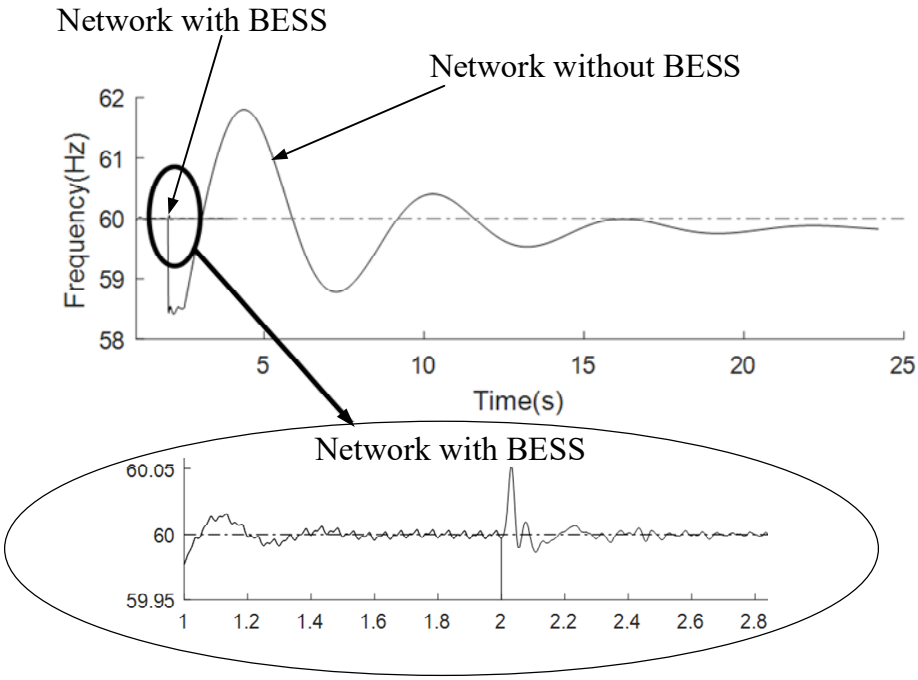

Figure 12: Frequency of load with and without BESS following load variation at second 2

Figure 13 demonstrates the voltage of the load with and without BESS following changing load at second 2. It is clear that the network with BESS can maintain the voltage on the reference level as well as damp out the oscillations after load variations. But the network without BESS is not able to keep the voltage on the nominal value and the voltage alters from the nominal value following load variation at second 2. Furthermore, the network without BESS comprises larger oscillations in the voltage.

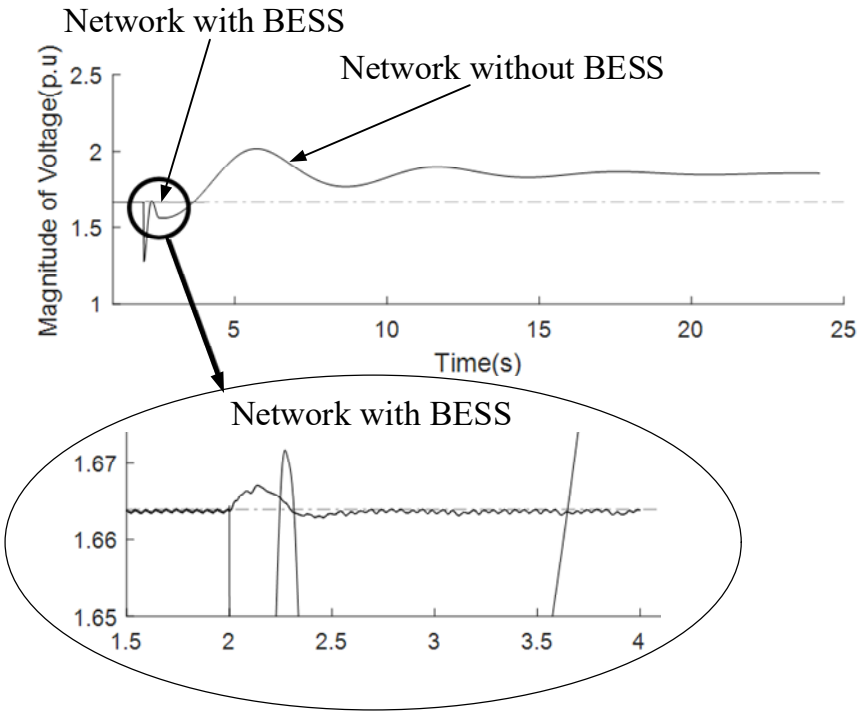

Figure 13: Voltage of load with and without BESS following load variation at second 2

Figure 14 shows frequency of the load with and without BESS following wind speed alteration at second 2. It is clear that the network with BESS can successfully fix the frequency on the set point level following wind speed variation at second 2. But the network without BESS cannot keep the frequency on the nominal level and the frequency increases following disturbance. Moreover, the oscillations of frequency in the network with BESS are rapidly damped out.

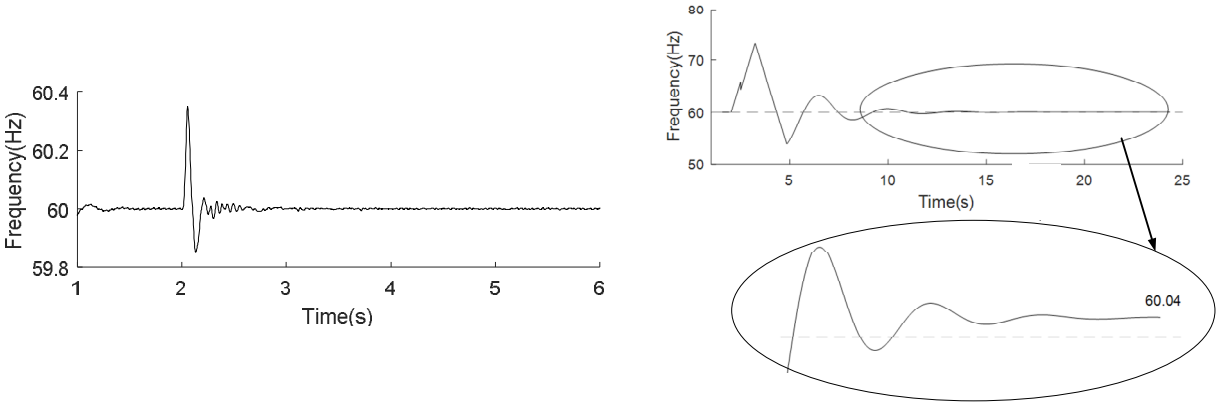

A: Network with BESS B: Network without BESS

Figure 14: Frequency of the load with and without BESS following wind speed variation at second 2

Figure 15 depicts voltage of the load with and without BESS following wind speed variation at second 2. It is confirmed that the network with BESS can successfully keep the voltage on the nominal value and it can efficiently damp out the oscillations. On the other hand, the network without BESS cannot fix voltage on the nominal level and is not able to damp out the oscillations efficiently.

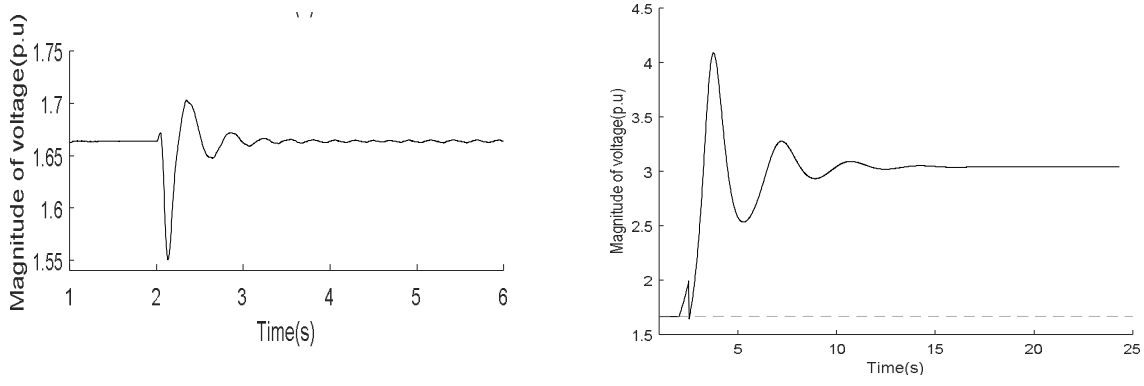

A: Network with BESS B: Network without BESS

Figure 15: Voltage of the load with and without BESS following wind speed variation at second 2

5.5. Operation with and without supplementary stabilizers

In order to demonstrate the impacts of supplementary stabilizers on the proposed control structure, operation of the network with and without supplementary stabilizers is simulated and compared. With the purpose of dynamic stability studies, a single-phase short circuit on load 2 with duration of 0.3 seconds is applied and simulated. Figures 16 and 17 show the frequency and voltage of load following single-phase short circuit. It is demonstrated the control loops with stabilizers can rapidly damp out the oscillations, while the control loops without stabilizers comprise large oscillations. It is also confirmed that both the frequency and voltage drive back to the nominal levels following disturbance. This issue emphasizes on precious of the introduced strategy for decentralized frequency-voltage control.

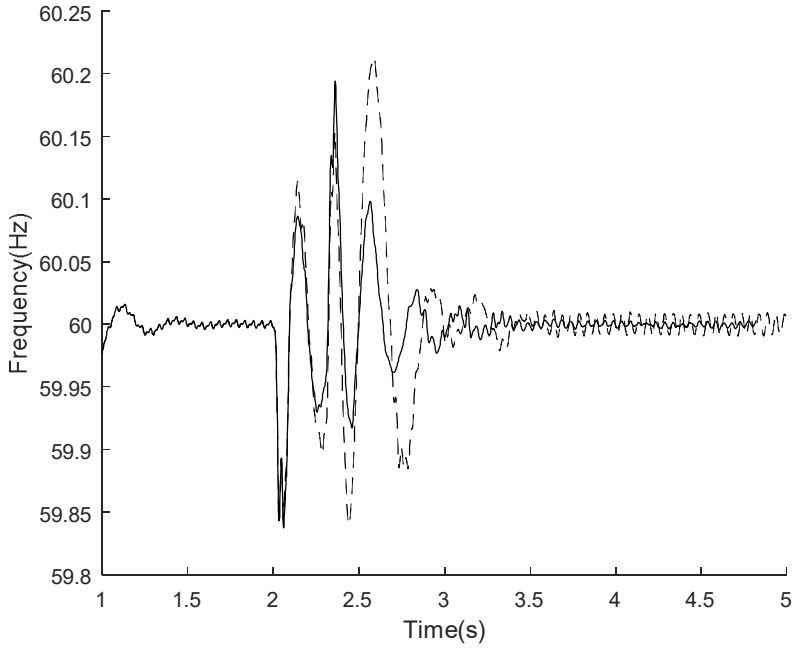

Figure 16: Frequency of the load following disturbance
Solid line: with stabilizer; dashed line: without stabilizer

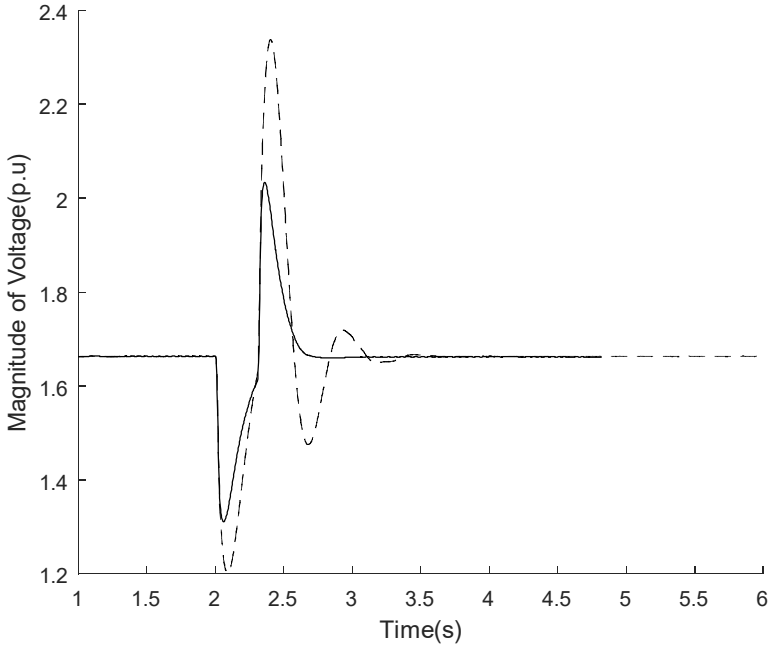

Figure 17: Magnitude of voltage of the load following disturbance
Solid line: with stabilizer; dashed line: without stabilizer

6. Conclusions

This paper introduced an advanced control strategy on battery energy storage system (BESS) for frequency control, voltage regulation, and stability enhancement at the same time. The proposed method was simulated and discussed on a standalone network including wind turbine-load-BESS. All the parameters of the controllers and stabilizers were optimally tuned by PSO algorithm. The simulation results demonstrated that the proposed control structure was able to control both frequency and voltage independent of each other. The results verified that the proposed control strategy could alter the frequency while the voltage was kept on the reference level. As well, the proposed control structure could efficiently change the voltage magnitude while it maintained the frequency on the set point level. Operation of the network under variable wind speed and variable load was also investigated. It was demonstrated that the proposed control structure was able to control both the frequency and voltage under variable wind speed

and variable load demand. The impacts of BESS on operation of the network was also discussed and simulated. It was addressed that the network without BESS could not keep the frequency and voltage on the nominal levels following disturbances. On the other hand, the network with BESS could successfully control both the frequency and voltage and set them on the reference levels following disturbance. Eventually, the impacts of supplementary stabilizers on the network stability were investigated. It was verified that the control loops with supplementary stabilizers could significantly damp out the oscillations and improve the network stability, while the control loops without stabilizers showed large amplitude oscillations.

Acknowledgements

J.P.S. Catalão acknowledges the support by FEDER funds through COMPETE 2020 and by Portuguese funds through FCT, under Projects SAICT-PAC/0004/2015 - POCI-01-0145-FEDER-016434, POCI-01-0145-FEDER-006961, UID/EEA/50014/2013, UID/CEC/50021/2013, UID/EMS/00151/2013, and 02/SAICT/2017 - POCI-01-0145-FEDER-029803, and also funding from the EU 7th Framework Programme FP7/2007-2013 under GA no. 309048.

References

[1] Zhang X, Yuan Y, Hua L, Cao Y, Qian K. On Generation Schedule Tracking of Wind Farms With Battery Energy Storage Systems. IEEE Transactions on Sustainable Energy. 2017;8(1):341-53.

[2] S. Sawyer aKR. Global Wind Report–Annual Market Update 2015. Global Wind Energy Council (GWEC)2015.

[3] Suh J, Yoon DH, Cho YS, Jang G. Flexible Frequency Operation Strategy of Power System With High Renewable Penetration. IEEE Transactions on Sustainable Energy. 2017;8(1):192-9.

[4] Bornapour M, Hooshmand R-A, Khodabakhshian A, Parastegari M. Optimal stochastic scheduling of CHP-PEMFC, WT, PV units and hydrogen storage in reconfigurable micro grids considering reliability enhancement. Energy Conversion and Management. 2017;150(Supplement C):725-41.

[5] Chen F, Li F, Wei Z, Sun G, Li J. Reliability models of wind farms considering wind speed correlation and WTG outage. Electric Power Systems Research. 2015;119(0):385-92.

[6] Moradi J, Shahinzadeh H, Khandan A, Moazzami M. A profitability investigation into the collaborative operation of wind and underwater compressed air energy storage units in the spot market. Energy. 2017;141(Supplement C):1779-94.

[7] Archer CL, Simão HP, Kempton W, Powell WB, Dvorak MJ. The challenge of integrating offshore wind power in the U.S. electric grid. Part I: Wind forecast error. Renewable Energy. 2017;103:346-60.

[8] Simão HP, Powell WB, Archer CL, Kempton W. The challenge of integrating offshore wind power in the U.S. electric grid. Part II: Simulation of electricity market operations. Renewable Energy. 2017;103:418-31.

[9] Tabar VS, Jirdehi MA, Hemmati R. Energy management in microgrid based on the multi objective stochastic programming incorporating portable renewable energy resource as demand response option. Energy. 2017;118 (1)(1): 827–39.

[10] Årdal AR, Undeland T, Sharifabadi K. Voltage and frequency control in offshore wind turbines connected to isolated oil platform power systems. Energy Procedia. 2012;24:229-36.

[11] Elmorshedy M, Allam S, Shobair AI, Rashad EM. Voltage and frequency control of a stand-alone wind-energy conversion system based on PMSG. Conference Voltage and frequency control of a stand-alone wind-energy conversion system based on PMSG. IEEE, p. 1-6.

[12] M. Chinchila SA, and J. C. Burgos. Control of permanent-magnet generators applied to variable-speed windenergy systems connected to the grid,". IEEE Transactions on Energy Conversion. 2006;21:130-5.

[13] Chinchilla M, Arnaltes S, Burgos JC. Control of permanent-magnet generators applied to variable-speed wind-energy systems connected to the grid. IEEE Transactions on energy conversion. 2006;21(1):130-5.

[14] Herrera D, Galván E, Carrasco JM. Method for controlling voltage and frequency of the local offshore grid responsible for connecting large offshore commercial wind turbines with the rectifier diode-based HVDC-link applied to an external controller. IET Electric Power Applications: Institution of Engineering and Technology; 2017. p. 1509-16.

[15] M. Davari aYM. Robust DC-link voltage control of a full-scale PMSG wind turbine for effective integration in DC grids,". IEEE Transactions on Power Electronics 2017;32:4021-35.

[16] X. Yuan FW, D. Boroyevich, Y. Li, and R. Burgos. DC-link voltage control of a full power converter for wind generator operating in weak-grid systems,". IEEE Transactions on Power Electronics. 2009;24:2178-92.

[17] M. E. Haque MN, and K. M. Muttaqi. A novel control strategy for a variable-speed wind turbine with a permanent-magnet synchronous generator,". IEEE Transactions on Industry Applications. 2010;1:331-9.

[18] Y. Kim MK, E. Muljadi, J. Park, and Y. Kang. Power smoothing of a variable-speed wind turbine generator in association with the rotor speed–dependent gain. IEEE Transactions on Sustainable Energy. 2016;8(3):990 - 9.

[19] A. Kassem aSZ. Load parameter waveforms improvement of a stand-alone wind-based energy storage system and Takagi-Sugeno fuzzy logic algorithm. IET Renewable Power Generation,. 2014;8:775-85.

[20] Wang Caisheng aMHN. Power management of a stand-alone wind/photovoltaic/fuel cell energy system. IEEE Transactions on Energy Conversion. 2008;23:957-67.

[21] Hemmati R. Optimal design and operation of energy storage systems and generators in the network installed with wind turbines considering practical characteristics of storage units as design variable. Journal of Cleaner Production. 2018;185:680-93.

[22] Hemmati R. Technical and economic analysis of home energy management system incorporating small-scale wind turbine and battery energy storage system. Journal of Cleaner Production. 2017;159:106-18.

[23] Fang Q, Berger CM, Menzler NH, Bram M, Blum L. Electrochemical characterization of Fe-air rechargeable oxide battery in planar solid oxide cell stacks. Journal of Power Sources. 2016;336:91-8.

[24] Kerdphol T, Qudaih Y, Watanabe M, Mitani Y. RBF neural network-based online intelligent management of a battery energy storage system for stand-alone microgrids. Energy, Sustainability and Society. 2016;6(1):5.

[25] Reza Hemmati NA. Advanced control strategy on battery storage system for energy management and bidirectional power control in electrical networks. Energy. 2017;138:520-8.

[26] Matlab Simulink software-Wind Turbine Asynchronous Generator in Isolated Network.

[27] Sang LQ, Takao M, Kamada Y, Li Qa. Experimental investigation of the cyclic pitch control on a horizontal axis wind turbine in diagonal inflow wind condition. Energy. 2017;134:269-78.

[28] Boubaker S. Identification of nonlinear Hammerstein system using mixed integer-real coded particle swarm optimization: application to the electric daily peak-load forecasting. Nonlinear Dynamics. 2017;90(2):797-814.

[29] Niknam T. A new fuzzy adaptive hybrid particle swarm optimization algorithm for non-linear, non-smooth and non-convex economic dispatch problem. Applied Energy. 2010;87(1):327-39.

[30] Parsopoulos KE, Vrahatis MN. Particle swarm optimization method for constrained optimization problems. Intelligent Technologies–Theory and Application: New Trends in Intelligent Technologies. 2002;76(1):214-20.

[31] Bai Q. Analysis of particle swarm optimization algorithm. Computer and information science. 2010;3(1):180.

[32] Clerc M. Particle swarm optimization: John Wiley & Sons, 2010.